Highlights

Improvement of syngas quality from two-stage downdraft wood gasification through steam and oxygen injection

A. Rouanet, H. Jeanmart

- Experiments of oxy-steam gasification were run on a two-stage downdraft gasifier.
- Syngas LHV is increased by +65% when replacing secondary air by oxygen.
- Oxygen raises the oxidation zone temperature, but steam compensates this effect.
- Steam enhances carbon conversion. Steam and oxygen increase the cold gas efficiency.
- Oxy-steam gasification yields more Class III and IV tars than air gasification.

Improvement of syngas quality from two-stage downdraft wood gasification through steam and oxygen injection

A. Rouanet, H. Jeanmart

[a]*Institute of Mechanics, Materials and Civil Engineering, Université catholique de Louvain, Place du Levant, 2, Louvain-la-Neuve, 1348, Belgium*

Abstract

The transition from fossil fuels to clean energy sources requires the supply of gaseous fuels from renewable origin for a number of applications. Such applications include in particular high-temperature heat for industries, and Combined Heat and Power (CHP) for flexible, decentralized power production. Gasification of lignocellulosic biomass is a good candidate to this end, converting solid biomass such as wood residues into a more versatile and CO_2-neutral gaseous fuel. Today, the use of syngas remains limited due to its relatively low energy density and challenges related to its residual tar content.

To improve the quality of syngas on these two aspects, we have studied the injection of steam and oxygen in a pilot two-stage downdraft gasifier. Replacing secondary air by oxygen enhances the Lower Heating Value (LHV) by 65%, while steam injection boosts the H_2/CO ratio and damps the temperature rise due to oxygen. The gasification efficiency is enhanced by both oxygen and steam. As a drawback, oxy-steam conditions yield more Class IV tars in the syngas. The combined use of oxygen and steam can enhance the volumetric power of syngas-based CHP engines, and provide a sustainable fuel for high-temperature industrial applications.

In future research, longer runs should be done to confirm the effects of steam and oxygen on conversion efficiency. The injection of steam and oxygen at the primary stage should also be studied. The presented results will help choosing whether to use oxygen and steam in downdraft gasification applications, and support the validation of numerical models.

Keywords:
biomass, downdraft, gasification, steam, oxygen, tar

Email address: arnaud.rouanet@uclouvain.be (A. Rouanet)

1. Introduction

Gasification of lignocellulosic biomass is an effective way to extend its use as a renewable energy source, by converting it into a more versatile gaseous fuel. Synthetic gas, or syngas, produced by biomass gasification, can provide a sustainable and carbon-neutral alternative to natural gas in a number of its current applications. However, syngas has two main technical limitations: its low energy density and residual tar content. Autothermal air gasification yields more than 50% of inert components in the syngas, mainly nitrogen, which dilute it and reduce its Lower Heating Value (LHV). Tar, hydrocarbons that can harmfully condense in downstream equipment, must be removed in a syngas cleaning step.

Downdraft gasifiers are particularly adequate for decentralized energy production through Combined Heat and Power (CHP) or small industrial applications, owing to their simple design and their small to medium capacity of up to $2\,\mathrm{MW}_{th}$. Among downdraft gasifier types, the two-stage concept is especially promising for its very low tar content of less than $100\,\mathrm{mg/Nm^3}$, 10 times lower than with traditional single-stage gasifiers. Examples of two-stage designs have been proposed by Bui et al. [1] and Martínez et al. [2], using a single fixed bed and a staged air injection in the porous bed. Brandt et al. [3] proposed a different approach, using an externally heated pyrolysis and only secondary air injection to sustain volatiles oxidation and char gasification. The design used in the present study was presented in [4], and combines both approaches by separating the pyrolysis and reduction beds with a staged air injection in gaseous zones located on top of each bed.

To improve the quality of syngas from autothermal gasification, a possible direction is the use of alternative gasification agents, in particular oxygen and steam. The use of oxygen, instead of air, can efficiently increase syngas LHV by reducing the dilution due to nitrogen. This is particularly relevant in the context of an increasing penetration of electrolysis for H_2 production from intermittent renewable power, where oxygen could be locally available as a by-product of this process. Steam could also enhance the gasification process, and can be produced using waste heat recovery from the hot syngas flow or a CHP engine exhaust.

To better understand the potential of oxy-steam gasification for syngas quality improvement, we have run experiments with oxygen and steam injection at the secondary stage of a pilot two-stage downdraft wood gasifier of $250\,\mathrm{kW}_{th}$. Regression models based on the experimental results are used to identify the individual impacts of steam injection, air enrichment and other secondary parameters.

The experimental results presented in this paper have two objectives. For existing or future applications of autothermal downdraft gasification, the drawn observations can be used to support the choice of whether or not to use steam and/or oxygen. The development of numerical models of gasifiers is an essential tool to further improve them, and the presented results can be used to help validate such models.

The theoretical effects of steam and oxygen on staged downdraft gasification are reviewed in Section 2, based on existing real-scale experimental results and lab-scale theory of tar reforming. The experimental set-up and experimental conditions are described in Section 3, and Section 4 presents the experimental results, summarized with the help of regression models and discussed in the perspective of the main syngas applications.

2. Theory

Prior knowledge on the impacts of steam and oxygen on downdraft wood gasification is described in this section. The first part covers existing experimental results on steam and/or oxygen injection in staged downdraft gasifiers. The second part digs into the theoretical mechanisms of *in-situ* tar reduction, and the potential effects of steam and oxygen on the efficiency of tar reforming.

2.1. Impacts of steam and oxygen on staged downdraft gasification

Experimental studies involving simultaneous injection of air, steam and oxygen in two-stage downdraft gasifiers are rare, and often focus on the production of hydrogen rather than a high LHV and low tar content. Furthermore, none of the gasifier designs used in the reviewed studies does include a physical separation of the biomass and char beds and an intermediate oxidation zone: all of them are based on a staged air injection in a continuous porous biomass bed.

With air and saturated steam in a dual-fired downdraft gasifier, Ram et al. [5] found that a Steam-to-Biomass mass Ratio (SBR) of around 0.2 maximized the syngas H_2 content (27.2%) and Higher Heating Value (HHV) (6.3 MJ/Nm^3). Jarungthammachote and Dutta [6] also investigated air-steam gasification in a two-stage gasifier, and similarly reported that SBR=0.2 yielded more H_2 (up to 16.6%) and a higher HHV (up to 5.3 MJ/Nm^3) compared to the situation with air only. They simultaneously observed an increase in the tar content, explained by the temperature reduction at the location of the steam injection, which negatively affected tar thermal cracking. In these studies, the focus on HHV instead of LHV induces a bias in favour of H_2: water condensation enthalpy is usually not recovered in CHP and industrial burners, and H_2 has a higher HHV but a lower LHV than CO.

Under similar conditions with air and steam in a 50 kW two-stage downdraft gasifier, de Sales et al. [7] found that steam injection resulted in a higher H_2 concentration (up to 20%) but a lower syngas LHV (below 4 MJ/Nm^3), due to the resulting increase in the air-fuel Equivalence Ratio (ER). They also observed that steam injection with air reduced the particle matter concentration (-50% from 102 to 53 mg/Nm^3), but increased the tar content (+69% from 54 to 92 mg/Nm^3) due to a lower temperature inside the gasifier. Using a combination of oxygen and steam, they reported a LHV up to 8.4 MJ/Nm^3 and observed that the use of O_2 mitigated the negative impact of steam on tar content.

Sandeep and Dasappa [8] used oxygen and large amounts of superheated steam (830°C, SBR between 0.5 and 1.7) in a staged open-top gasifier, for hydrogen production. They reported a syngas LHV up to 8.9 MJ/Nm^3, and observed that as the amount of steam increased, the syngas H_2 content was raised up to 50%, at the expense of a lower syngas LHV.

Only partial agreement was found on the effects of oxygen and steam on syngas LHV and tar content in staged downdraft gasifiers. The diversity of operating conditions, such as the secondary-to-primary O_2 ratio and the Equivalence Ratio (ER), can explain some of the differences observed. Results are often presented in a way that is difficult to generalize to other similar installations. Overall, existing studies show that oxy-steam gasification boosts the syngas LHV, but the individual effects of oxygen and steam are not clearly distinguished as no experiment with oxygen only was found. Steam injection increases the H_2 concentration, but opposite observations exist on its effect on the syngas LHV. Finally, the respective effects

of oxygen and steam on tar were not studied in much depth, and seem to depend much on the temperature conditions in the gasifier.

2.2. Tar definition and mechanisms of in-situ tar reduction

Tar from biomass gasification is usually defined as follows: *all organics boiling at temperatures above that of benzene should be considered as tar* [9]. As it is not clear whether benzene itself is included in this definition, it will be treated separately and explicitly included or excluded in this study.

Tar species are usually classified as primary, secondary and tertiary tar, following the definition given in the review of Milne and Evans [9]. Primary tars are oxygenated compounds resulting from the pyrolysis of cellulose, hemicellulose and lignin, such as levoglucosan, glycolaldehyde, guaiacol and furfurals. Secondary tars are composed of a diversity of phenolics and olefins produced by cracking and oxidation of primary tars in mild conditions (500-800°C). Tertiary tars result from reactions of primary and secondary tars at higher temperature (above 800°C). They are composed of substituted (methyl derivatives) and unsubstituted aromatics and polyaromatic hydrocarbons (PAHs): benzene, toluene, naphthalene, indene, methylnaphthalene and PAHs with 3 or more rings. Primary and secondary tars can be thermally cracked into CO, H_2 and light gases, while tertiary tars species are refractory and much more difficult to destroy.

A complementary classification of tar species was proposed by Kiel et al. [10], consisting of 5 classes based on tar species condensation behavior and water solubility:

- Class I: GC-undetectable. Heaviest molecules that condense at very high temperature.
- Class II: Heterocyclic compounds containing O and/or N atoms, mainly phenolics or nitrogenous aromatics. They condense at moderate temperatures, between 50 and 100°C for concentrations from 10 to 1000 $\mathrm{mg/Nm^3}$. Their polarity induces a high water solubility, increasing the complexity of waste-water treatment from the cleaning system.
- Class III: Aromatics derivatives of benzene, such as toluene and xylene. They are not polar and do not condense thanks to their very low dew point (below 0°C up to 10 $\mathrm{g/Nm^3}$).
- Class IV: Light PAHs of 2-3 rings, from naphthalene to phenanthrene. Non-polar, they condense at moderate temperatures similar to Class II species.
- Class V: heavy PAHs of 4-7 rings, from fluoranthene to coronene. They condense at high temperature even when in very low concentration (above 100°C at 0.1 $\mathrm{mg/Nm^3}$).

The mechanism of tar reduction and destruction inside a gasifier can be roughly split in two main parts: the homogeneous conversion of primary and secondary tars into light gases and tertiary tars (aromatics and Polyaromatic Hydrocarbons – PAHs), and the decomposition of tertiary tars by heterogeneous reactions over the char bed acting as a catalyst. This is particularly applicable in a two-stage gasifier, where the two parts occur, respectively, within the oxidation and the reduction zones. The destruction of tar inside a gasifier is favoured by three factors: temperature, oxygen and steam, in that order of importance. High temperature

partial oxidation is essential for efficient tar reforming, especially for the conversion of primary and secondary tars [11].

Steam can affect both parts of that process. By releasing $H^{\bullet}$, $O^{\bullet\bullet}$ and $OH^{\bullet}$ radicals at high temperature, it favors the conversion of substituted aromatics and phenols into benzene and light PAHs, and hence reduces the yield of heavy PAHs of which phenol is the main precursor. In particular, the presence of many $H^{\bullet}$ radicals help to saturate intermediate radicals to single ring aromatics (benzene) and light hydrocarbons (C_2, C_3), avoiding their recombination into polyaromatic compounds [12].

Steam can also indirectly affect the heterogeneous conversion of heavy PAHs by maintaining the catalytic activity of char, through the gasification of char and coke deposits by $OH^{\bullet}$ radicals. Under a sufficient temperature (700–900°C), tar heterogenous conversion occurs through 1) adsorption on the char active sites, 2) polymerization (coke formation) and 3) gasification. This efficiently decomposes aromatics and heavy tar, but char activity rapidly decreases due to micropores blocking by coke deposition: steam can help maintain char activity by supporting the gasification step [13].

Both effects of steam on tar do require a sufficient temperature, which is the primary factor affecting tar cracking efficiency. Most of the experimental results on tar reforming with steam found in the literature used externally heated reactors, maintained at temperatures between 700 and 900°C to isolate the chemical effect of steam. However, experimental research on autothermal staged downdraft gasifiers with steam have reported a higher tar concentration, due to a negative impact on the reaction temperature [6, 7].

3. Material and Methods

This section describes the experimental set-up and the experimental conditions. The gasifier design, syngas cleaning and steam and oxygen injection systems are described first, together with the equipment used for syngas analysis and the tar sampling line. Then, the factors of interest and main response variables of the experimental plan are detailed, as well as the methodology used to select valid steady-state operating points.

3.1. Experimental set-up

The experimental gasifier is a pilot two-stage downdraft gasifier based on the NOTAR© technology, extensively described by Berger [4]. This gasifier design is structured in three main sections (Figure 1):

1. the pyrolysis zone, where biomass is dried and converted into char and volatile compounds by an oxidative pyrolysis;
2. the oxidation zone, where volatiles are oxidized and cracked in homogeneous reactions at high temperature;
3. the reduction zone, where heterogeneous char gasification reactions convert the gaseous products into useful CO and H_2.

Air injection is split into two stages: primary air at the top of the pyrolysis zone and secondary air in the oxidation zone. At both stages, air is injected through four nozzles evenly distributed around the gasifier. The independent control of the pyrolysis, and the high-temperature homogeneous oxidation zone where tars are cracked and oxidized by the secondary air injection, are the key features enabling a very low tar content below 100 mg/Nm^3.

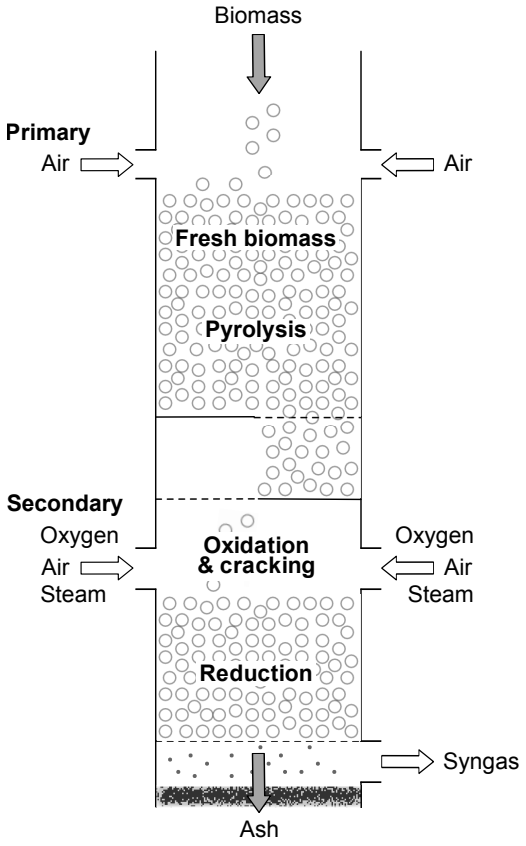

Figure 1. The two-stage gasifier design.
Pyrolysis volatiles are oxidized and cracked in the hot gas-phase zone [4].

The nominal biomass consumption is 50 kg/h, corresponding to 250 kW of biomass LHV and up to 175 kW of syngas LHV. Wood chips are loaded in a hopper from which they are fed to the gasifier using a worm screw, via an airlock to prevent any escape of syngas. Temperature is measured at 20 points located in spiral along the gasifier height: 11 in the pyrolysis zone, 3 in the oxidation zone and 8 in the reduction zone. At the bottom of the gasifier, the reduction bed lies on an ash rack which can be actuated to help dislocate the bed and extract the ashes when pressures losses build up.

Syngas cleaning is required to protect any downstream piping or equipment from clogging due to the condensation of remaining tar compounds. Cooling and cleaning of raw syngas is done in four main steps at the gasifier outlet (Figure 2). Fine ash in suspension are first removed by a dust cyclone (4). Syngas is then mixed with water in a Venturi scrubber right upon entering a counter-current heat exchanger (5) where water and tar condense out of the cooled syngas stream. The following wet cyclone (6) ensures that fine droplets of water entrained by the flow are removed, and the granular filter (7) acts as a final trap for remaining solid particles or droplets. The clean syngas flow is then measured with an orifice flow meter, before flaring or use.

The steam injection system consists of an electric steam generator of 22 kW producing up to 25 kg/h of saturated steam, followed by a steam superheater. Steam flow regulation is done with an orifice flow meter and a control valve. Insulation and trace heating are used on

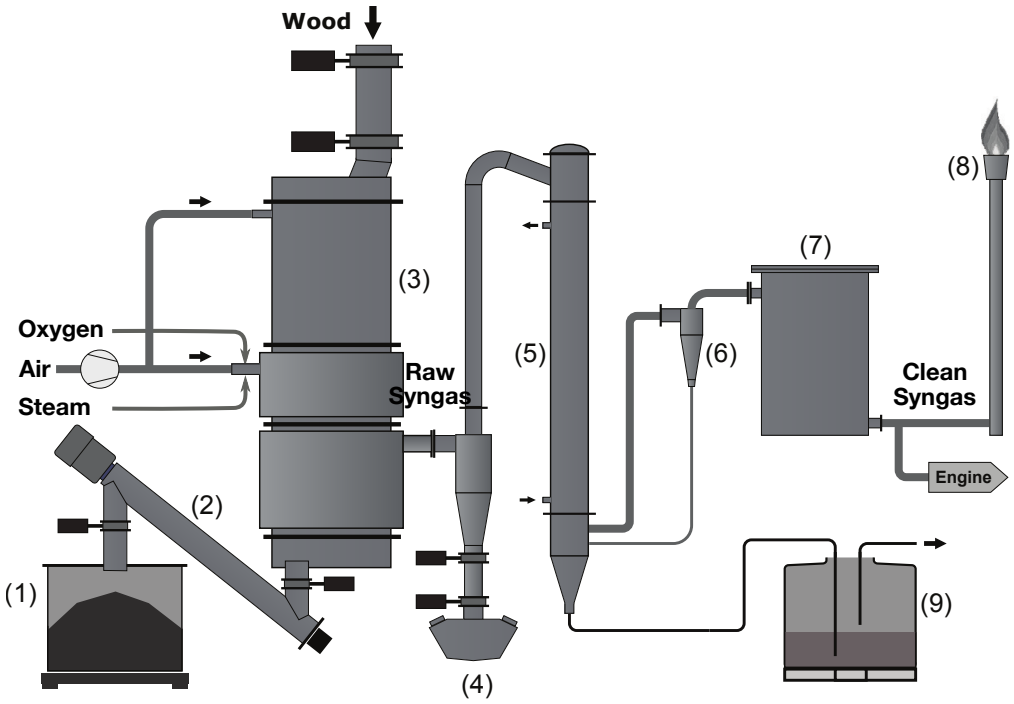

Figure 2. Gasifier and syngas cleaning: (1-2) ash tank and extraction, (3) gasifier, (4) cyclone and fine ash collector, (5) condenser, (6) wet cyclone, (7) granular filter, (8) flare and (9) water decantation tank [4].

the steam lines to maintain the steam temperature until the injection nozzles to the oxidation zone.

Oxygen is produced with a Pressure-Swing Adsorption (PSA) oxygen generator, with an oxygen purity of $x_{O_2,\text{oxygen}} = 95\%$. Steam, air and oxygen are injected at the secondary stage through 4 injection nozzles spread around its circumference. Air and steam are mixed inside the nozzles, ensuring their homogeneous mixing before injection, while oxygen is injected through concentric nozzles for safety reasons.

Syngas composition after cleaning is determined using an on-line gas analyser. CO, H_2 and CH_4 are quantified with a Siemens ULTRAMAT 23 non-dispersive infrared sensor (NDIR), which also contains a paramagnetic sensor used to detect the presence of O_2. A thermal conductivity detector (TCD) Siemens CALOMAT 62 is coupled to measure the H_2 concentration. N_2 is calculated by difference as $100\% - [CO] - [CO_2] - [CH_4] - [H_2]$, and actually includes all other inert species like Ar.

Tars are sampled following the Tar Protocol guidelines [14]: hot syngas flows through a series of impingers filled with isopropanol, first at ambient temperature, then at $-20°C$ to ensure complete tar condensation. After sampling, the isopropanol solution is analyzed by GCMS, seeking 84 tar species including alcohols, acids, aldehydes, ketones, phenols, guaiacols, furans, aromatics, nitrogenous aromatics, anisoles, PAHs, terpenes and sugars. The list of species actually found in the samples in quantity higher than their Limit of Quantitification (LOQ) is given in Table E.9. The volume of dry syngas is measured with a volumetric meter during sampling, with temperature and pressure correction, and used to convert the concentrations in mg/l to their equivalent mg/Nm^3 of dry syngas (see Table C.7 for details).

3.2. Experimental conditions

Wood chips of 10-40 mm with less than 10% moisture are used as feedstock for all experiments. Two different batches were used over the experimental campaigns, with very similar properties. Their detailed composition is given in Table A.4 in the Appendix.

Experimental conditions are detailed in Table 1. The two primary factors of interest are the Steam-to-Oxygen molar ratio SOR (Eq. (1)) and the equivalent air enrichment x_{O_2} [%] (Eq. (2)). The SOR is varied from 0 to 2 and represents the steam flow normalized by the total input of O_2 from air and oxygen flows. Oxygen injection at the secondary stage results in an increase of x_{O_2}, ranging from 21% with air to 47% when secondary air is replaced by oxygen. Intermediate values correspond to a mixture of secondary air and oxygen.

Secondary control factors are the total equivalent air flow $Q_{\text{air,eq}}$ [Nm^3/h] (Eq. (3)), the secondary-to-primary O_2 ratio β (Eq. (4)) and the injection temperature of steam T_{st}. $Q_{\text{air,eq}}$ corresponds to the air flow containing an equivalent amount of O_2 as the combined air and oxygen flows, and should primarily control the gasifier power. It was varied between 60 and 70 Nm^3/h. β represents the ratio of secondary and primary O_2 flow from the combined air and oxygen flows. It is a control variable that must be adjusted during operation to maintain the pyrolysis front stability, and is usually between 2.0 and 2.5. Finally, steam was either saturated (LT, 100-150°C) or superheated (HT, 250-500°C).

$$\text{SOR} = \frac{\dot{n}_{\text{H2O}_\text{g}}}{\dot{n}_{O_2}} = \frac{\dot{m}_{\text{steam}}/M_{\text{steam}}}{x_{O_2,\text{air}} Q_{\text{air,eq}}/V_0} \tag{1}$$

$$x_{O_2} = \frac{x_{O_2,\text{air}} Q_{\text{air,primary}} + x_{O_2,\text{air}} Q_{\text{air,secondary}} + x_{O_2,\text{oxygen}} Q_{\text{oxygen,secondary}}}{Q_{\text{air,primary}} + Q_{\text{air,secondary}} + Q_{\text{oxygen,secondary}}} \tag{2}$$

$$Q_{\text{air,eq}} = Q_{\text{air,primary}} + Q_{\text{air,secondary}} + Q_{\text{oxygen,secondary}} \frac{x_{O_2,\text{oxygen}}}{x_{O_2,\text{air}}} \tag{3}$$

$$\beta = \frac{x_{O_2,\text{air}} Q_{\text{air,secondary}} + x_{O_2,\text{oxygen}} Q_{\text{oxygen,secondary}}}{x_{O_2,\text{air}} Q_{\text{air,primary}}} \tag{4}$$

3.3. Response variables

The primary response variables are the syngas composition (CO, H_2, CO_2, CH_4) and LHV on dry basis, after cooling (Eq. (5)). The syngas H_2/CO ratio is observed, as it is strongly influenced by the injection of steam. The Energy Density ED (Eq. (6)) and Adiabatic Flame Temperature AFT (Eq. (7)) of the stoichiometric air-syngas mixture are computed as secondary responses. The ED controls the volumetric power of an Internal Combustion Engine (ICE), relevant for CHP applications. The AFT gives an idea of the flame temperature that can be reached, useful for high-temperature burners for industrial applications. In Equation (7), n_i and $h_{s,i}$ are the amount [kmol] and sensible enthalpy [kJ/kmol] of each product of the complete stoichiometric combustion of one kmol of syngas, and $V_0 = \frac{RT_0}{p_0} = 22.414\,\text{Nm}^3/\text{kmol}$ is the normal volume of 1 kmol under NTP conditions of 0°C and 1 bar.

The gasifier power is observed, both in terms of biomass consumption P_{biomass} and syngas production P_{syngas}. The air-fuel Equivalence Ratio (ER) is computed (Eq. (8)), as well as the Cold Gas Efficiency CGE (Eq. (9)) and the Carbon Conversion Efficiency CCE (Eq.

2nd stage	Run ID	SOR	x_{O_2} %	$Q_{air,eq}$ Nm^3/h	β	T_{steam} °C	Wood batch	Duration min
Air	air60_A	0.00	21.0	59.4	2.26		1	79
	air60_B	0.00	21.0	58.6	1.97		2	74
	air70_A	0.00	21.0	68.8	2.49		2	108
	air70_B	0.00	21.0	69.3	2.99		2	90
Air-steam	air70_st10LT	0.86	21.0	69.2	1.94	104	1	58
	air60_st20LT	2.00	21.0	59.5	2.00	103	1	99
	air60_st20HT	2.03	21.0	58.8	2.00	271	1	67
Air-O_2	air$O_2$65	0.00	28.2	64.8	1.63		2	108
	air$O_2$70	0.00	32.3	70.0	2.55		2	70
O_2	$O_2$60	0.00	47.3	59.8	2.53		2	100
	$O_2$70	0.00	47.5	70.0	2.55		2	78
O_2-steam	$O_2$60_st10LT_A	1.09	44.0	60.6	2.07	117	2	72
	$O_2$60_st10LT_B	0.99	47.2	59.8	2.52	146	2	68
	$O_2$60_st10HT	0.99	43.8	60.2	2.04	399	2	82
	$O_2$60_st20LT	1.98	47.3	60.1	2.53	127	2	97
	$O_2$60_st20HT	1.97	47.5	60.3	2.55	460	2	67
	$O_2$70_st20LT	1.97	47.4	70.3	2.53	134	2	91

Table 1. Experimental conditions of the 17 experimental points.

(10)). As the injection of oxygen can result in a problematic temperature increase, the average temperature in the oxidation zone $T_{oxi,avg}$ is also monitored. Finally, the amount and composition of tars and lighter hydrocarbons are of primary interest in this study.

$$\mathrm{LHV} = x_{CO}\mathrm{LHV}_{CO} + x_{H_2}\mathrm{LHV}_{H_2} + x_{CH_4}\mathrm{LHV}_{CH_4} \quad (5)$$

$$\mathrm{ED} = \mathrm{LHV}/\left(1 + \frac{0.5x_{CO} + 0.5x_{H_2} + 2x_{CH_4}}{x_{O_2,air}}\right) \quad (6)$$

$$\mathrm{AFT} \equiv \mathrm{LHV} = \sum_{i\in P} n_i h_{s,i}(\mathrm{AFT})/V_0 \quad (7)$$

$$\mathrm{ER} = \frac{x_{O_2}Q_{air,eq}/V_0}{\left(1+\frac{y}{4}-\frac{x}{2}\right)\dot{m}_{biomass,daf}/M_{CH_yO_xN_z}} \quad (8)$$

$$\mathrm{CGE} = \frac{P_{syngas}}{P_{biomass,wb}} = \frac{Q_{syngas}\mathrm{LHV}}{\dot{m}_{biomass,wb}\mathrm{LHV}_{biomass,wb}} \quad (9)$$

$$\mathrm{CCE} = \frac{\dot{n}_{C,syngas}}{\dot{n}_{C,biomass}} = \frac{\left(x_{CO}+x_{CO_2}+x_{CH_4}\right)Q_{syngas}/V_0}{\dot{m}_{biomass,daf}/M_{CHyO_xN_z}} \quad (10)$$

Due to its scale and substantial mass of concrete, the gasifier has a big inertia and several hours of operation are required to reach stable steady-state operating points. Experimental results presented in this paper are based on stable operation periods of a duration varying between 58 and 108 minutes. These periods were selected based on the stability of the syngas

composition and LHV. Results are averaged over each considered stable period, and used to fit regression models including second-order and interaction terms on x_{O_2} and SOR, and first-order terms on $Q_{air,eq}$ and β. The steam temperature T_{st} was not found to have any statistically relevant impact and was discarded from the models. The obtained regression models are used to synthesize experimental results and observe trends.

4. Results and Discussion

Experimental results and the associated regression models are presented and discussed in this section. First, the syngas composition, H_2/CO ratio, LHV, ED and AFT are observed. The gasifier power, CGE and CCE are analyzed, followed by the impact of steam and oxygen on the temperature in the oxidation zone. Tars are finally discussed. The complete results of syngas composition, LHV, biomass and syngas flow and power, and efficiency, are provided in Tables B.5 and B.6 in the Appendix.

In all figures and tables presented in this section, regression-based results are computed using $Q_{air,eq} = 65$ and $\beta = 2.25$ if not otherwise specified. In the graphs, the following code applies to the markers used to represent experimental results: $Q_{air,eq}$=60 (circle), 65 (diamond) or 70 Nm^3/h (square); x_{O_2}=21% (empty), 32% (empty with a dot) or 47% (full); SOR=0 (dark red), 1 (medium red) or 2 (light red).

4.1. Syngas composition and H_2/CO ratio

The volume composition of dry syngas is given in Table 2. The concentrations of H_2, CO, CO_2 and N_2 are shown in Figures 3 and 4 for different values of the SOR, respectively with air and oxygen at the secondary stage. These values are computed using the regression model fitted on the experimental data, including 2^{nd} order and interaction terms for SOR and x_{O_2}, and 1^{st} order terms for $Q_{air,eq}$ and β.

Steam injection boosts the production of H_2 and CO_2 at the expense of CO. This effect is due to the Water-Gas Shift reaction (Eq. (11)) being shifted towards the products, according to Le Chatelier's principle. The use of oxygen, instead of air, reduces the concentration of N_2 in the syngas, scaling up H_2, CO, CO_2 and CH_4 accordingly.

$$CO + H_2O \rightleftharpoons CO_2 + H_2 \tag{11}$$

The shift of syngas from CO towards H_2 with steam injection translates into a linear increase of the H_2/CO ratio: from almost 1.0 without steam up to 2.0 at SOR = 2 (Figure 5). Experimental results are fitted by a regression model based only on SOR and x_{O_2}, as there is no statistically valid impact of the other factors. The H_2/CO ratio is a relevant metric for some applications: a high value is desirable for the synthesis of advanced biofuels such as methane or methanol, or for H_2 production. Moreover, the combustion behaviors of H_2 and CO are different, and their relative share can affect the flame properties such as the laminar flame speed and ignition temperature [15].

Beyond these primary observations of the dry syngas composition, the impacts of oxygen and steam can be better observed and understood by avoiding the effect of the variable syngas dilution. The normalized composition $x_{i,norm}$ [%] is calculated by dividing the volume concentration by the total amount of carbon in the syngas (Eq. (12)). The amount of carbon

2nd stage	x_{O_2} %	SOR	CO %	H_2 %	CH_4 %	CO_2 %	N_2 %
		0	18.4	16.8	0.73	12.2	51.9
Air	21	1	15.2	21.1	0.90	14.6	48.1
		2	12.4	23.6	1.00	17.2	45.7
Air-O_2	32	0	24.2	24.5	1.21	14.9	35.1
		0	29.1	29.2	1.21	18.6	21.9
O_2	47	1	23.5	33.9	1.42	21.7	19.4
		2	18.4	36.8	1.54	24.9	18.3

Table 2. Syngas composition, predicted by the regression model built on experimental results. $Q_{\text{air,eq}} = 65$, $\beta = 2.25$.

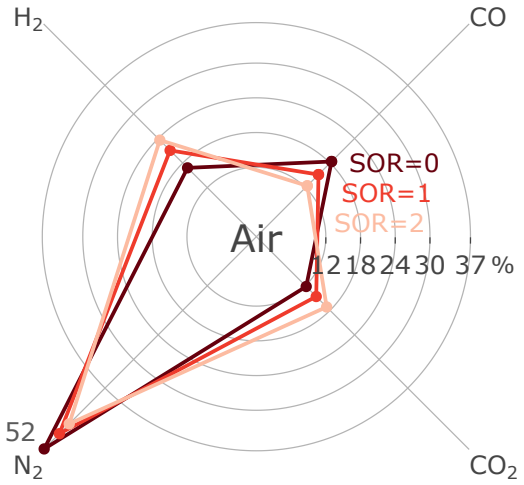

Figure 3. Dry syngas composition with air *(regression model with $Q_{air,eq} = 65$ and $\beta = 2.25$).*

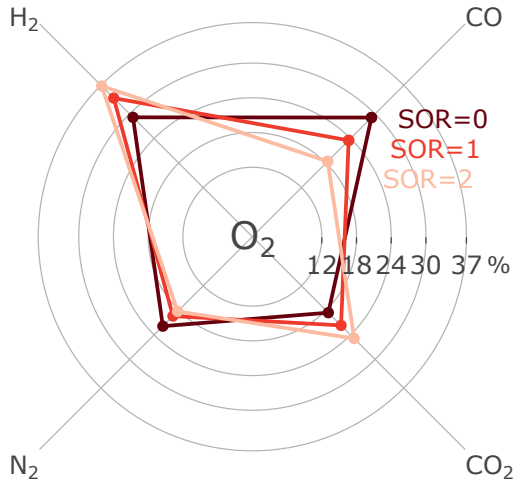

Figure 4. Dry syngas composition with oxygen *(regression model with $Q_{air,eq} = 65$ and $\beta = 2.25$).*

is representative of the amount of biomass converted into syngas, disregarding the part of carbon lost in the ashes.

$$x_{i,\text{norm}} = \frac{x_i}{x_{\text{CO}} + x_{\text{CO}_2} + x_{\text{CH}_4}} \tag{12}$$

With oxygen, more H_2 and CO and less CO_2 are produced than with air, in normalized composition (Figure 6). The lower dilution reduces the amount of energy lost as syngas sensible enthalpy, and less complete combustion to CO_2 and H_2O is therefore required to sustain the process energy needs. This results in a lower Equivalence Ratio, and a higher production of CO and/or H_2.

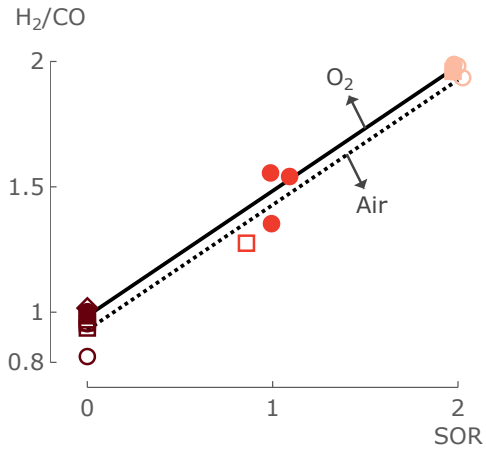

Figure 5. The H_2/CO ratio increases linearly with the SOR, doubling from 1.0 to 2.0. *Regression (lines) and experimental points (markers).*

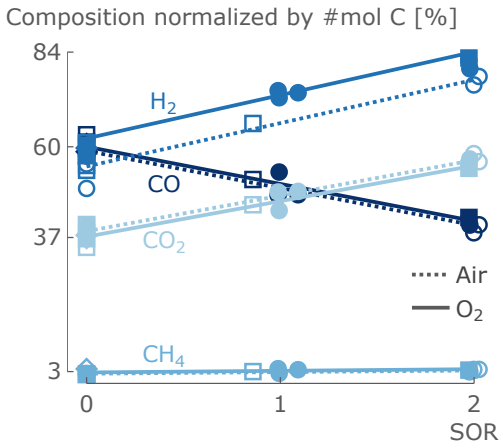

Figure 6. Syngas composition normalized by the amount of carbon: experimental results and regressions.

4.2. LHV, Energy Density and Adiabatic Flame Temperature

The volume-based LHV of dry syngas is the best metric to characterize its intrinsic energy content. It is preferable to HHV as in most applications of syngas, the latent enthalpy of vaporization of water is not valorized. The use of HHV would artificially favor a H_2-rich syngas, as H_2 has a higher HHV but lower LHV than CO. The use of a volume basis (MJ/Nm^3) is more relevant than a mass basis (MJ/kg): as syngas is a gaseous fuel, its storage, transport and control are mainly constrained by its volume rather than weight. The use of a mass basis would also artificially favor a H_2-rich syngas, due to its low density, while mass is not a real issue when dealing with gaseous fuels.

Thanks to the reduced dilution and higher production of H_2 and CO, syngas LHV is increased up to +65% when replacing air by oxygen at the secondary stage: from 4.40 to 7.26 MJ/Nm^3 (Figure 7 and Table 3). The effect of air enrichment is quadratic: LHV is already 6.14 MJ/Nm^3 at $x_{O_2} = 32\%$ (+40%), which corresponds to a partial secondary air enrichment of around 40% O_2.

Steam seems to have a slightly positive impact on the LHV with air (up to around 4.50 MJ/Nm^3), but this very small effect is not statistically representative. With oxygen, steam reduces the syngas LHV, especially at SOR=2 where it drops to 6.85 MJ/Nm^3 (−5%). Compared to the reference air conditions, the LHV improvement with oxygen and SOR=2 is +56%. This effect of steam is explained by the higher amount CO_2 produced by the water-gas-shift reaction (Eq. (11)), which dilute the syngas.

From the perspective of syngas applications, specific metrics can be more adequate than the LHV, such as the Energy Density (ED) and Adiabatic Flame Temperature (AFT) of the air-syngas stoichiometric mixture. The ED is proportional to the volumetric power that can be obtained when burning syngas in an internal combustion engine, for CHP applications. The AFT is relevant for processes requiring a very high flame temperature, such as glass furnaces that operate at up to 1600°C [16].

Replacing secondary air by oxygen also yields a higher ED (+26% from 2.3 to 2.9 MJ/Nm^3)

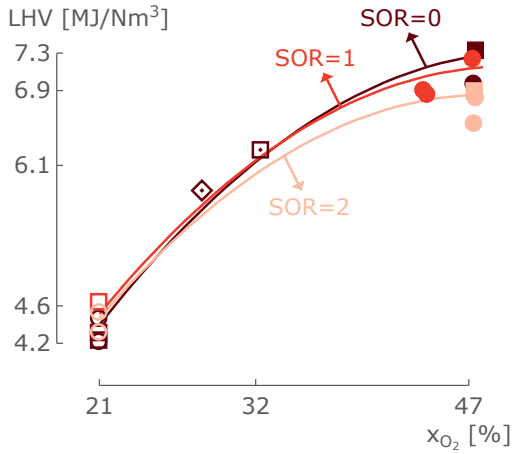

Figure 7. Syngas LHV is increased to 7.3 MJ/Nm^3 (+65%) when replacing secondary air by oxygen, lowered to 6.9 MJ/Nm^3 (+56%) with SOR = 2.
Lines: regression model ($Q_{air,eq} = 65$, $\beta = 2.25$). Markers: experimental points.

and AFT (+350 K from 1820 to 2170 K) (Figures 8 and 9 and Table 3). For a given value of LHV, both the ED and AFT are lower with steam, as steam injection slightly increases the production of CH_4 (Table 2). Due to its high LHV, this small increase has a substantial effect on its share in the total syngas LHV, which rises from 6% to 9%. This results in a comparatively lower ED, as the ED/LHV ratio of CH_4 is about 3 times lower than CO and H_2. Due to the combined effect of a lower LHV and higher CH_4 content, the ED and AFT obtained with oxygen and SOR = 2 is equivalent to the values that would be obtained using a mixture of air and oxygen such that $x_{O_2} \approx 36\%$, which corresponds to a secondary air enrichment of about 50% O_2.

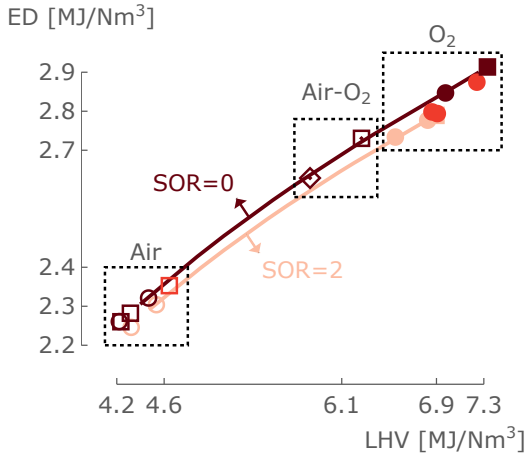

Figure 8. Energy Density of the stoichiometric air-syngas mixture.
Regression (lines) and experimental points (markers).

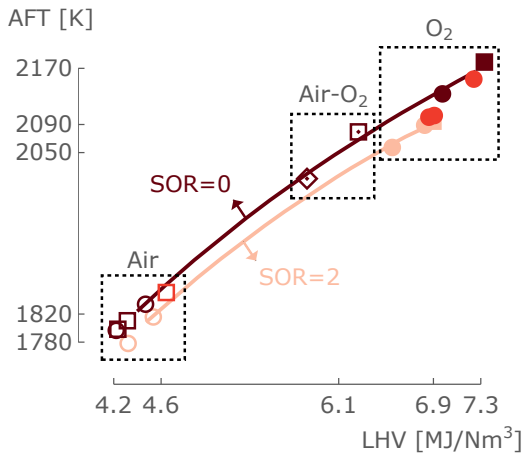

Figure 9. Adiabatic Flame Temperature of the stoichiometric air-syngas mixture.
Regression (lines) and experimental points (markers).

2^{nd} stage	x_{O_2} %	SOR	LHV MJ/Nm^3	ED MJ/Nm^3	AFT K	ED/LHV %
		0	4.40	2.31	1824	52.4
Air	21	1	4.52	2.32	1829	51.3
		2	4.47	2.29	1808	51.2
Air-O_2	32	0	6.14	2.70	2055	43.9
		0	7.26	2.90	2166	40.0
O_2	47	1	7.13	2.85	2134	40.0
		2	6.85	2.78	2088	40.6
CO			12.63	3.73	2663	29.6
H_2			10.79	3.19	2524	29.6
CH_4			35.79	3.40	2327	9.5

Table 3. LHV, ED and AFT of syngas (regression model) and of the individual species CO, H_2 and CH_4.

4.3. Gasifier power and efficiency

The gasifier input power, which corresponds to the biomass flow rate, is primarily proportional to the equivalent air flow $Q_{\text{air,eq}}$ (Figure 10). It also increases when replacing air by oxygen, as a result of the higher reactivity in the oxidation and reduction zones. A substantial variability of the biomass flow is observed between runs under similar conditions. This is partly due to the uncertainty on the wood chips consumption, which is not directly measured, but computed based on the duration of successive hopper loads and the average mass per hopper. The high gasifier inertia and long residence time of solid particles increase the uncertainty on the value of biomass consumption to consider, especially on relatively short runs of 1-2 hours. This uncertainty on the input power in turn affects the CGE and CCE values.

The actuation frequency of the ash removal rack plays an important role on the Carbon Conversion Efficiency (CCE), as shown in Figure 11: a high frequency increases the extraction of unconverted carbon, lowering the CCE. This frequency is controlled during operation to maintain acceptable pressure losses through the reduction bed. The injection of steam appears to enhance the carbon conversion: results with SOR = 2 are associated with the lowest actuation frequency and the highest CCE. Two points have a very low CCE, probably due to a too frequent ash rack actuation leading to a loss of carbon and an over-consumption of wood; they are considered outliers.

A higher CCE directly translates into a higher Cold Gas Efficiency (CGE) (Figure 12). Furthermore, the use of oxygen (full markers) yields a higher CGE than equivalent results with air (empty markers). This improvement results from the lower Equivalence Ratio with oxygen: as less biomass is burnt to sustain the process energy needs, a higher share of its LHV remains available in the syngas LHV. Combining the effects of steam on the CCE, and of steam and oxygen on the ER, the best CGE are obtained under oxy-steam conditions: all lie between 70% and 73%, while most air-only, air-steam and O_2-only conditions yield a CGE between 61% and 70%.

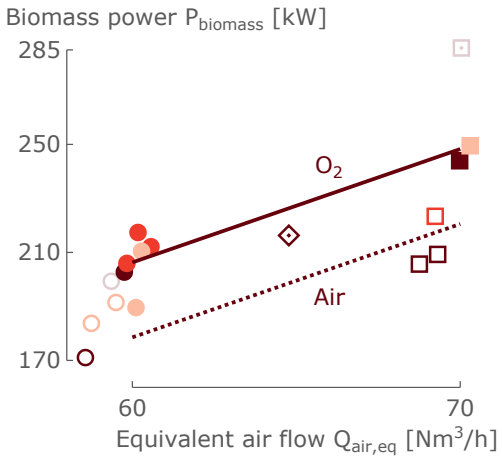

Figure 10. Biomass consumption mainly depends on $Q_{\text{air,eq}}$ and x_{O_2}. *Lines: regression (*SOR $= 0$, $\beta = 2.25$*). Markers: experimental points.*

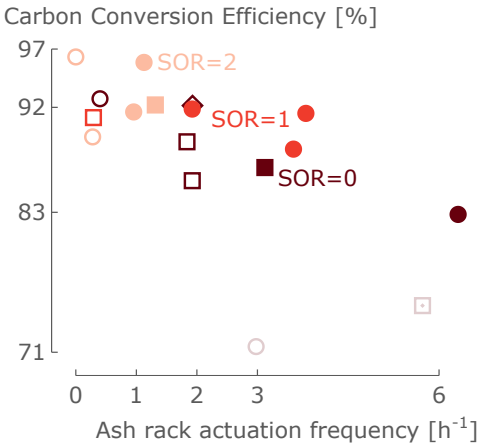

Figure 11. Carbon Conversion Efficiency is strongly influenced by the ash rack actuation frequency, and appears enhanced by steam injection.

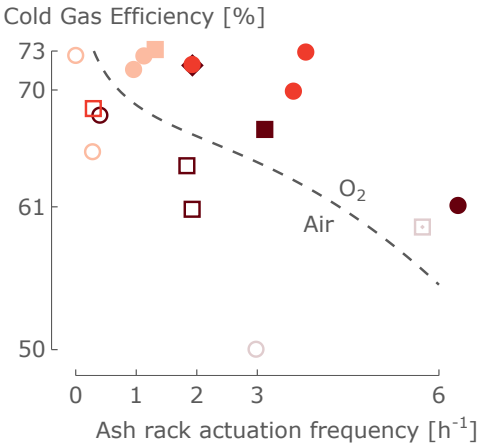

Figure 12. Cold Gas Efficiency is highest with a combination of oxygen and steam.

4.4. Temperature in the oxidation zone

The hottest zone of the gasifier is the oxidation zone, where the high temperature contributes to the efficiency of tar cracking. However, very high temperatures must be avoided as they can cause excessive mechanical wear to the concrete and stainless steel parts inside the gasifier.

Under air gasification, the average temperature in the oxidation zone $T_{\text{oxi,avg}}$ is around 980°C, with local peaks not exceeding 1020°C (Figures 13 and 14). The use of oxygen at the secondary stage causes a strong temperature rise, as the diluting effect of nitrogen is reduced: the average temperature increases up to 1190°C, with local peaks up to 1260°C. The fluctuations observed are due to the discontinuous transfer of char from the pyrolysis zone: when a large mass of fresh char falls to the reduction bed, the oxidation zone temperature

drops as the new char suddenly cools down the second stage. The oscillations are particularly strong using oxygen, as the lower dilution of the gaseous mixture implies a lower thermal inertia.

When adding steam to oxygen, it acts as a thermal damper, reducing $T_{\text{oxi,avg}}$ to around 1040°C at SOR = 2, with local peaks not exceeding 1100°C. This temperature is similar to the one obtained with a mixture of air and oxygen at $x_{O_2} \approx 30\%$. That cooling effect of steam, mainly observed with oxygen, is due to two effects: the enthalpy required to heat it up to the local temperature, and the endothermic nature of water-gas shift and steam gasification reactions.

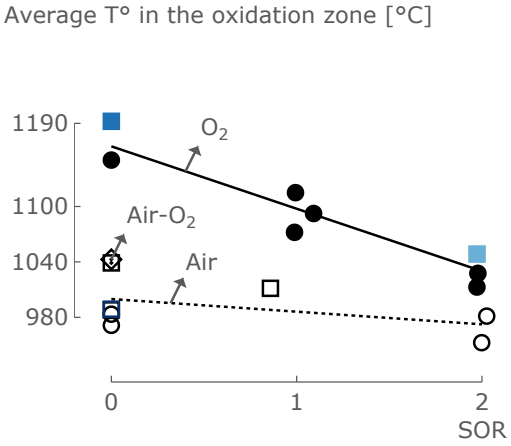

Figure 13. The average temperature in the oxidation zone increases by +200°C using O_2, but this effect is compensated by the injection of steam. *Regression (lines) and experimental points (markers).*

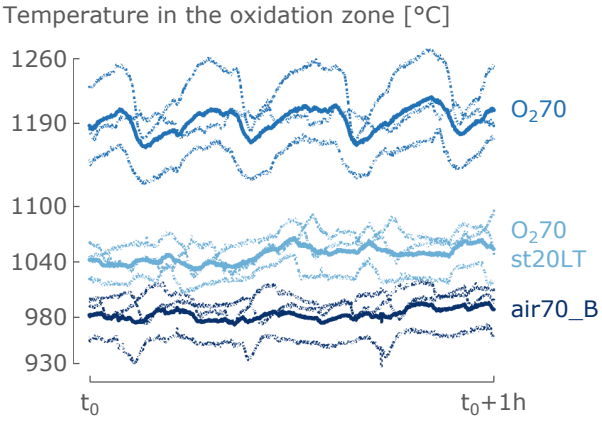

Figure 14. Temperature fluctuations are much stronger with oxygen, with local peaks up to 1260°C. *Light dotted lines: individual thermocouples. Dark solid lines: average values.*

4.5. Tar amount and composition

Among the 84 species looked for in the GCMS analysis of the tar samples, only 15 were found in a representative quantity, higher than their Limit Of Quantification (LOQ). The LOQ of most tar species is 1 mg/l, in the isopropanol solution. The equivalent value, in mg/Nm^3 of dry syngas, depends on the conversion factor specific to each sampling conditions. For most runs, the equivalent LOQ of most species is between 1.8 and 2.5 mg/Nm^3 of dry syngas (Table C.7).

In the reference air conditions, the total concentration of tar species heavier than benzene lies around 30 mg/Nm^3 (Figure 15). Adding steam to air does not have any distinguishable effect on the total tar concentration. Replacing air by O_2 increases tar concentration to 45-60 mg/Nm^3. Adding steam to oxygen results in a strong increase of the tar concentration: doubling it to 120 mg/Nm^3 at SOR=2.

Benzene concentration is much higher than all other tar species, which is why it is treated separately. In the reference air conditions, its concentration is in the range 100–200 mg/Nm^3. It increases to 300–400 mg/Nm^3 under oxygen gasification, and up to 450–650 mg/Nm^3 with oxygen and SOR = 2. No clear effect of steam injection with air is identified.

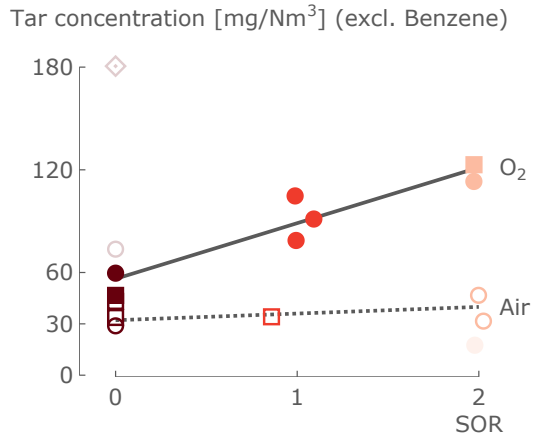

Figure 15. Concentration of tars heavier than benzene increases from 30 mg/Nm^3 with air up to 120 mg/Nm^3 in oxy-steam conditions.
Lines: regression model $f(\mathrm{SOR}, x_{\mathrm{O_2}}, x_{\mathrm{O_2}} \times \mathrm{SOR})$.
Markers: experimental points.

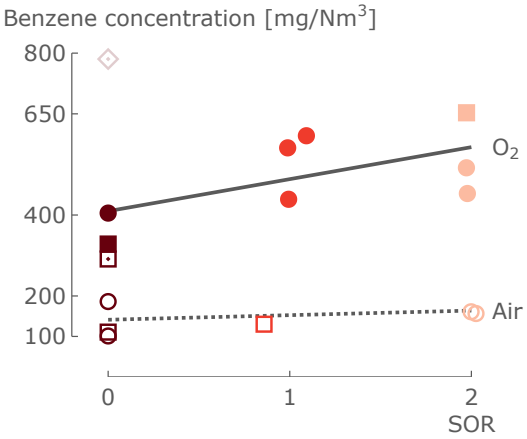

Figure 16. Concentration of benzene is 3–5 times higher than other tar species. It is highest under oxy-steam conditions.
Lines: regression model $f(\mathrm{SOR}, x_{\mathrm{O_2}}, x_{\mathrm{O_2}} \times \mathrm{SOR})$.
Markers: experimental points.

For a more detailed understanding of how tar production is affected by varying conditions, tar classes II, III and IV are separately analyzed in Figures 17 and 18. Observing only the tar concentration in mg/Nm^3 can hide effects that are solely related to the variable syngas dilution, with more or less N_2. To avoid this effect and get more insight into the production of tar, the amount is normalized by the syngas LHV, expressed in mg/MJ. The concentration of tar in the dry syngas is given for each class in Table D.8 in the Appendix.

Class IV tars found in the samples are mainly composed of naphthalene (more than 90%), with some acenaphthylene, acenaphthene and phenanthrene. They are tertiary species produced by the thermal cracking of secondary tars, and are problematic due to their relatively high dew point, as introduced in Section 2.2.

When added to air, steam decreases the production of tertiary tar: from 2–4 mg/MJ down to 1 mg/MJ (Figure 17). This effect is probably due to the presence of more $H^\bullet$ and $OH^\bullet$ radicals, which prevent the formation of PAHs by saturating aromatic rings and reforming their phenolic precursors. On the other hand, the replacement of air by oxygen slightly increases class IV tar production (5–6 mg/MJ), despite an increase of more than 200°C of the average temperature in the oxidation zone. When adding steam to oxygen, the class IV tar production further increases to 8–12 mg/MJ at SOR=1 and up to 15 mg/MJ at SOR=2. That effect is correlated with a lower $T_{\mathrm{oxi,avg}}$ resulting from the injection of steam.

These last trends are unexpected, as steam and oxygen are in theory beneficial to an efficient tar cracking. The main explanation is that the use of oxygen can imply a less efficient mixing between O_2 and the pyrolysis volatiles in the oxidation zone, as the volume flow from the secondary nozzles is 5 times lower than with air. This can leave more areas in very rich conditions at a very high temperature, favorable to the recombination of hydrocarbons in polyaromatic rings. With oxygen only, this effect appears partly offset by the higher average temperature favorable to tar cracking. The addition of steam reduces the average temperature in the oxidation zone (as discussed in Section 4.4), affecting the efficiency of

thermal tar cracking.

Class III tar species are essentially benzene (94–100%), with some toluene (up to 6%) and small amounts of styrene (max 0.5%). These species have a very low dew point and are relatively easy to burn, and are thus not harmful for most applications. Yet, they are relevant to monitor as their presence can affect the syngas combustion properties, such as ignition timing and flame radiation.

The production of Class III species is 7–40 times higher than Class IV species, with at least 25 mg/MJ under air gasification conditions (Figure 18). They are affected in a quite similar way as what is observed for Class IV species, as they are also tertiary products: their production increases slightly when switching from air to oxygen (from 25–45 to 45–60 mg/MJ), and adding steam worsens that effect by lowering the oxidation zone temperature (up to 100 mg/MJ). Regarding air-steam conditions, the effect of steam is not clear but it tends to slightly increase the production of benzene; this is an expected effect, as steam favors single-ring aromatics.

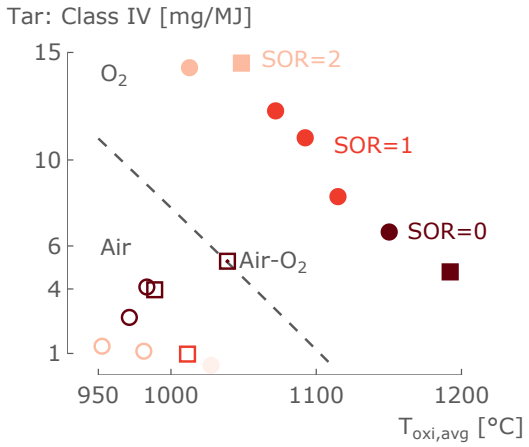

Figure 17. Up to 5 times more class IV tars are produced in oxy-steam conditions. Steam addition to air does reduce class IV tar production.

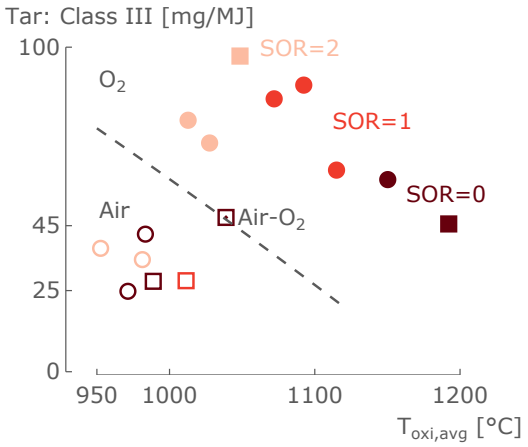

Figure 18. Class III tars are affected by oxygen in a similar way as Class IV species.

Class II tar species are mainly phenol (42% or more), cresol (up to 32%) and xylenol (max 15%) in the present results. These species are problematic on two levels: their high dew point, and their polarity which makes the waste-water treatment very complex, as explained in Section 2.2. They are produced by the conversion of primary pyrolysis products, and most of them should normally be destroyed or converted to tertiary tars in the oxidation zone. Their presence can be due to a too low pyrolysis front, resulting in incompletely pyrolysed biomass falling to the reduction zone, some secondary species thereby avoiding the oxidation zone.

In all experiments with O_2 or air-O_2, the amount of class II tars is below 1 mg/MJ. They are only found in substantial quantity in some results of the first experimental campaign, studying the impact of steam addition with air. The highest amount (14 mg/MJ) is obtained without steam injection, down to 6 mg/MJ at SOR=2. This could indicate a positive effect of steam, favoring their reforming by providing many $H^\bullet$ and $OH^\bullet$ radicals. However, the

lowest amounts are also associated with a slightly higher and warmer pyrolysis front, which could be another explanation to the lower production of Class II tars. Overall, their amount is very low in almost all results, and no clear impact of steam and oxygen can be concluded.

5. Conclusion

An experimental study has been performed on the impacts of varying amounts of air, oxygen and steam injected at the secondary stage of a pilot two-stage downdraft gasifier. The primary effect of replacing secondary air by oxygen is to increase the syngas LHV, from 4.5 up to 7.3 MJ/Nm^3. This translates into a higher Energy Density (+26%) and Adiabatic Flame Temperature (+350 K) of the air-syngas stoichiometric mixture. This richer syngas can represent a sustainable alternative to gaseous fossil fuels for CHP applications or high-temperature industrial processes.

Using oxygen also raises the temperature in the oxidation zone of the gasifier, from 1000°C up to 1200°C, which can be harmful on the long term. Steam acts as a thermal damper, bringing the temperature back to more acceptable values with only a limited impact on the syngas LHV (-5% to 6.9 MJ/Nm^3). The steam present in the syngas condenses in the cleaning process, but it also increases the production of CO_2 which results in some dilution of the dry syngas.

On the efficiency level, the injection of steam appears to enhance the conversion of carbon, which is positive on two levels: it reduces the amount of solid residue, and improves the process efficiency. The use of oxygen instead of air further increases the Cold Gas Efficiency, by enabling a lower Equivalence Ratio. The combination of oxygen and steam therefore has the potential to produce a richer syngas, with a better process efficiency.

Oxy-steam gasification has a drawback: it increases the concentration of tar in the syngas, from 60 up to 120 mg/Nm^3. Class IV tars contribute to most of that increase, resulting in a higher tar dew point. However, such amounts of tars remain very low compared to most other gasifier types.

Considering their various impacts, the choice of whether to use oxygen and/or steam in two-stage downdraft gasification should be specific to each application, as trade-offs are required between their various effects and the cost of steam and oxygen production. In a future work, the energy balance of the gasifier under air, oxygen and oxy-steam conditions should be studied in the perspective of the overall process efficiency. Long-duration runs should also be performed to validate the effects observed on the conversion efficiency, based on a complete mass and energy balance. The injection of steam and oxygen at the primary stage of the gasifier should also be studied, as a next step towards an almost N_2-free syngas. Finally, the experimental results presented in this paper should be used to support the development and validation of numerical models of two-stage gasifiers.

6. Nomenclature

AFT	Adiabatic Flame Temperature of the air-fuel stoichiometric mixture
CCE	Carbon Conversion Efficiency
CGE	Cold Gas Efficiency
CHP	Combined Heat and Power
ED	Energy Density of the air-fuel stoichiometric mixture
ER	air-fuel Equivalence Ratio
LHV	Lower Heating Value
LOD	Limit Of Detection
LOQ	Limit Of Quantification
HHV	Higher Heating Value
SBR	Steam to Biomass mass ratio
SOR	Steam to Oxygen molar ratio
x_{O_2}	Molar fraction of O_2 in the combined air and oxygen flows
β	Secondary-to-primary O_2 ratio
$\dot{m}$	Mass flow [kg/h]
$\dot{n}$	Molar flow [kmol/h]
Q	Normal volume flow [Nm^3/h]
wb	Wet basis (as-received)
db	Dry basis
daf	Dry and ash-free

7. Acknowledgements

This research was conducted as part of the project ENERBIO, for which the authors acknowledge the financial support of the Fonds européen de développement régional (FEDER) and Service Public de Wallonie (SPW).

Appendix A. Feedstock characteristics

	1st batch	2nd batch	
Moisture	7.1	8.7	$\%_{wb}$
Ash	0.5	2.1	$\%_{db}$
C	51.4	49.5	$\%_{db}$
H	5.4	5.5	$\%_{db}$
N	0.16	0.20	$\%_{db}$
O (by difference)	42.5	42.7	$\%_{db}$
Formula (*daf*)	$CH_{1.25}O_{0.62}N_{0.003}$	$CH_{1.32}O_{0.65}N_{0.003}$	
H/C ratio (incl. moisture)	1.45	1.58	
LHV (dry basis)	18942	18197	kJ/kg_{db}

Table A.4. Composition and heating value of the two batches of wood chips used are very similar.

Appendix B. Experimental results

Run ID	CO %	H_2 %	CH_4 %	CO_2 %	N_2 %	H_2/CO	LHV MJ/Nm^3	ED MJ/Nm^3	AFT K
air60_A	18.6	15.3	0.65	11.7	53.9	0.82	4.22	2.26	1797
air60_B	18.3	17.4	0.79	12.2	51.3	0.95	4.47	2.32	1834
air70_A	17.8	17.0	0.65	12.3	52.2	0.96	4.31	2.28	1810
air70_B	17.7	16.6	0.58	12.4	52.7	0.94	4.23	2.26	1798
air70_st10LT	16.3	20.8	0.95	14.3	47.6	1.28	4.64	2.35	1851
air60_st20LT	11.6	22.9	1.08	17.7	46.7	1.98	4.32	2.25	1778
air60_st20HT	12.4	23.9	1.09	17.3	45.3	1.94	4.53	2.30	1816
air$O_2$65	22.6	22.9	1.41	14.4	38.6	1.02	5.83	2.63	2013
air$O_2$70	25.6	24.8	0.99	14.0	34.5	0.97	6.27	2.73	2079
$O_2$60	28.1	28.1	1.12	19.5	23.2	1.00	6.98	2.85	2134
$O_2$70	29.9	29.5	1.04	17.9	21.6	0.99	7.33	2.91	2179
$O_2$60_st10LT_A	21.5	33.2	1.57	21.9	21.7	1.54	6.86	2.80	2100
$O_2$60_st10LT_B	25.0	33.8	1.20	20.5	19.4	1.35	7.24	2.87	2155
$O_2$60_st10HT	21.4	33.3	1.68	21.8	21.6	1.56	6.91	2.79	2103
$O_2$60_st20LT	17.9	35.5	1.31	25.3	20.0	1.99	6.55	2.73	2057
$O_2$60_st20HT	18.8	36.8	1.37	24.8	18.2	1.96	6.83	2.78	2089
$O_2$70_st20LT	18.8	36.9	1.51	24.4	18.3	1.96	6.90	2.79	2095

Table B.5. Syngas composition, H_2/CO ratio, LHV, ED and AFT.

Run ID	$\dot{m}_{\text{biomass},wb}$ kg/h	Q_{syngas} Nm^3/h	P_{biomass} kW	P_{syngas} kW	CGE %	CCE %	ER	$T_{\text{oxi,avg}}$ °C
air60_A	41.2	85	199	100	50.0	71.5	0.34	971
air60_B	37.5	94	171	116	68.1	92.7	0.38	983
air70_A	45.1	110	206	132	64.2	89.0	0.38	988
air70_B	45.9	108	209	127	60.8	85.7	0.37	989
air70_st10LT	46.2	119	223	153	68.6	91.1	0.35	1011
air60_st20LT	39.6	104	191	125	65.2	89.5	0.35	953
air60_st20HT	38.0	106	184	134	72.7	96.3	0.36	981
air$O_2$65	47.5	96	216	155	71.9	92.2	0.34	1043
air$O_2$70	62.7	98	286	170	59.4	75.0	0.28	1039
$O_2$60	44.5	64	203	124	61.1	82.8	0.33	1150
$O_2$70	53.5	80	244	163	67.0	86.8	0.32	1192
$O_2$60_st10LT_A	46.5	80	212	153	72.0	91.9	0.32	1092
$O_2$60_st10LT_B	45.2	75	206	150	72.9	91.5	0.33	1115
$O_2$60_st10HT	47.7	79	217	152	69.9	88.4	0.31	1072
$O_2$60_st20LT	41.6	76	190	138	72.6	95.9	0.36	1028
$O_2$60_st20HT	46.2	79	210	151	71.6	91.6	0.32	1013
$O_2$70_st20LT	54.7	95	249	182	73.1	92.2	0.32	1049

Table B.6. Biomass and syngas flow and power, CCE, CGE, ER and average temperature in the oxidation zone.

Appendix C. Tar sampling conditions

Run ID	Duration min	Syngas volume Nm^3/h	Sample volume l	Conversion l/Nm^3
air60_A	51	0.16	0.47	2.96
air60_B	84	0.17	0.39	2.28
air70_B	38	0.18	0.38	2.13
air70_st10LT	67	0.17	0.40	2.37
air60_st20LT	78	0.18	0.40	2.26
air60_st20HT	76	0.18	0.41	2.29
air$O_2$65	84	0.11	0.46	4.22
air$O_2$70	42	0.20	0.46	2.29
$O_2$60	47	0.21	0.45	2.13
$O_2$70	40	0.17	0.40	2.39
$O_2$60_st10LT_A	42	0.17	0.42	2.50
$O_2$60_st10LT_B	61	0.11	0.37	3.53
$O_2$60_st10HT	63	0.26	0.48	1.84
$O_2$60_st20LT	58	0.26	0.50	1.91
$O_2$60_st20HT	58	0.25	0.48	1.91
$O_2$70_st20LT	63	0.28	0.51	1.83

Table C.7. Tar sampling conditions and conversion factors.

Appendix D. Tar concentration

	II		III		IV	
Run ID	Phenol mg/Nm^3	Others mg/Nm^3	Benzene mg/Nm^3	Others mg/Nm^3	Naphthalene mg/Nm^3	Others mg/Nm^3
air60_A	24.8	34.1	101.2	3.4	11.3	
air60_B	7.3		186.2	3.3	18.3	
air70_B	9.7		110.7	7.3	16.8	
air70_st10LT	14.1	15.5	130.2		4.5	
air60_st20LT	17.8	19.8	160.9	3.4	5.8	
air60_st20HT	12.1	14.4	156.6		5.0	
air$O_2$65	6.4		785.4	20.0	149.4	4.8
air$O_2$70	3.4		291.3	6.6	33.2	
$O_2$60	5.0		404.8	8.2	46.4	
$O_2$70	6.0		328.3	5.4	35.1	
$O_2$60_st10LT_A	5.5		595.9	10.1	73.1	2.6
$O_2$60_st10LT_B	7.8		438.9	10.9	60.1	
$O_2$60_st10HT	5.1		565.9	14.8	74.1	10.7
$O_2$60_st20LT	5.9		453.1	8.7	2.9	
$O_2$60_st20HT	3.4		516.7	12.3	87.8	9.7
$O_2$70_st20LT	4.9		652.6	18.0	90.5	9.5

Table D.8. Tar amount in the syngas, in mg/Nm^3, per tar class. Empty cells are <LOQ. The list of species included in "Others" can be found in Table E.9.

Appendix E. Tar species quantified by GCMS

Class	Type	CAS	Name	LOQ mg/l
II	Phenols	108-95-2	Phenol	1
		95-48-7	o-Cresol	1
		106-44-5	m/p-Cresol	2
		95-65-8	3,4-Xylenol	1
		105-67-9	2,4-Xylenol	1
	Ketones	765-70-8	3-methyl-1,2-cyclopentanedione	1
		10493-98-8	2-hydroxy-2-cyclopenten-1-one	1
III	Aromatics	71-43-2	Benzene	1
		108-88-3	Toluene	1
		100-42-5	Styrene	1
IV	PAHs	91-20-3	Naphthalene	1
		208-96-8	Acenaphthylene	1
		83-32-9	Acenaphthene	1
		85-01-8	Phenanthrene	1

Table E.9. List of tar species found in the samples in quantity above their Limit of Quantification (LOQ), from a total list of 84 potential species sought.

References

[1] T. Bui, R. Loof, S. C. Bhattacharya, Multi-stage reactor for thermal gasification of wood, Energy 19 (1994) 397–404. doi:10.1016/0360-5442(94)90118-X.

[2] J. D. Martínez, E. E. Silva Lora, R. V. Andrade, R. L. Jaén, Experimental study on biomass gasification in a double air stage downdraft reactor, Biomass and Bioenergy 35 (2011) 3465–3480. doi:10.1016/j.biombioe.2011.04.049.

[3] P. Brandt, E. Larsen, U. Henriksen, High tar reduction in a two-stage gasifier, Energy and Fuels 14 (2000) 816–819. URL: https://pubs.acs.org/doi/10.1021/ef990182m. doi:10.1021/ef990182m.

[4] B. Berger, Experimental and numerical investigation of a two-stage downdraft biomass gasification process, Ph.D. thesis, Université catholique de Louvain, 2018.

[5] N. K. Ram, N. R. Singh, P. Raman, A. Kumar, P. Kaushal, A detailed experimental analysis of air–steam gasification in a dual fired downdraft biomass gasifier enabling hydrogen enrichment in the producer gas, Energy 187 (2019) 115937. doi:10.1016/j.energy.2019.115937.

[6] S. Jarungthammachote, A. Dutta, Experimental investigation of a multi-stage air-steam gasification process for hydrogen enriched gas production, International Journal of Energy Research 36 (2012) 335–345. doi:10.1002/er.1795.

[7] C. A. V. B. de Sales, D. M. Y. Maya, E. E. S. Lora, R. L. Jaén, A. M. M. Reyes, A. M. González, R. V. Andrade, J. D. Martínez, Experimental study on biomass (eucalyptus spp.) gasification in a two-stage downdraft reactor by using mixtures of air, saturated steam and oxygen as gasifying agents, Energy Conversion and Management 145 (2017) 314–323. doi:10.1016/j.enconman.2017.04.101.

[8] K. Sandeep, S. Dasappa, Oxy-steam gasification of biomass for hydrogen rich syngas production using downdraft reactor configuration, International Journal of Energy Research 38 (2014) 174–188. doi:10.1002/er.3019.

[9] T. A. Milne, R. J. Evans, Biomass gasifier "tars": their nature, formation and conversion, 1998. URL: https://www.osti.gov/etdeweb/biblio/20008297. doi:10.1007/978-94-009-1559-6_64.

[10] J. Kiel, S. V. Paasen, J. Neeft, Primary measures to reduce tar formation in fluidised-bed biomass gasifiers, Technical Report, 2004. URL: http://www.ecn.nl/publicaties/PdfFetch.aspx?nr=ECN-C--04-014.

[11] Y. Zhang, S. Kajitani, M. Ashizawa, Y. Oki, Tar destruction and coke formation during rapid pyrolysis and gasification of biomass in a drop-tube furnace, Fuel 89 (2010) 302–309. doi:10.1016/j.fuel.2009.08.045.

[12] D. Feng, Y. Zhao, Y. Zhang, S. Sun, Effects of H2O and CO2 on the homogeneous conversion and heterogeneous reforming of biomass tar over biochar, International Journal of Hydrogen Energy 42 (2017) 13070–13084. doi:10.1016/j.ijhydene.2017.04.018.

[13] S. Hosokai, K. Norinaga, T. Kimura, M. Nakano, C. Z. Li, J. I. Hayashi, Reforming of volatiles from the biomass pyrolysis over charcoal in a sequence of coke deposition and steam gasification of coke, Energy and Fuels 25 (2011) 5387–5393. doi:10.1021/ef2003766.

[14] J. P. Neeft, H. A. Knoef, G. J. Buffinga, U. Zielke, K. Sjöström, C. Brage, P. Hasler, P. A. Smell, M. Suomalainen, M. A. Dorrington, C. Greil, Guideline for Sampling and Analysis of Tars and Particles in Biomass Producer Gases, Progress in Thermochemical Biomass Conversion (2002) 162–175. doi:10.1002/9780470694954.ch11.

[15] C. J. Sung, C. K. Law, Fundamental combustion properties of H2/CO mixtures: Ignition and flame propagation at elevated pressures, Combustion Science and Technology 180 (2008) 1097–1116. doi:10.1080/00102200801963169.

[16] M. Zier, P. Stenzel, L. Kotzur, D. Stolten, A review of decarbonization options for the glass industry, Energy Conversion and Management: X 10 (2021) 100083. URL: https://doi.org/10.1016/j.ecmx.2021.100083. doi:10.1016/j.ecmx.2021.100083.

List of Figures

List of Tables